

Research Article

Evolution of the Water Vapor Plume over Eastern Europe during Summer 2010 Atmospheric Blocking

Sergei A. Sitnov,¹ Igor I. Mokhov,¹ and Anthony R. Lupo²

¹ A. M. Obukhov Institute of Atmospheric Physics, Russian Academy of Sciences, Pyzhevsky 3, Moscow 119017, Russia

² Department of Soil, Environmental and Atmospheric Sciences, University of Missouri, 302 ABNR Building, Columbia, MO 65211, USA

Correspondence should be addressed to Sergei A. Sitnov; sitnov@ifaran.ru

Received 28 August 2013; Revised 2 November 2013; Accepted 9 December 2013; Published 10 February 2014

Academic Editor: Stephen J. Colucci

Copyright © 2014 Sergei A. Sitnov et al. This is an open access article distributed under the Creative Commons Attribution License, which permits unrestricted use, distribution, and reproduction in any medium, provided the original work is properly cited.

We present an analysis of water vapor (WV) plume evolution over Eastern Europe (EE) during atmospheric blocking in the summer of 2010, carried out on the basis of satellite (MODIS and MLS instruments), aerological, and NCEP/NCAR reanalysis data. The obtained results show that the development of blocking was accompanied by the development of a positive anomaly of total column water vapor (TCWV) content over the northern part of EE. Local TCWV content from 28 July to 6 August 2010 reached 3.35 cm, a value that exceeded by 3.3 times its content before the block. The surplus of WV was mainly conditioned by the advection of WV due to transfer of moist air from the Atlantic Ocean and the Mediterranean Sea into northern EE and also due to increased evaporation from the surface enriched with water due to increased temperature and wind. We hypothesize that the influx of latent heat in the block area can contribute to the energy supply of the blocking anticyclone and prolong the existence of block. Strong humidification of the troposphere and some dehumidification of the lower stratosphere during the block were accompanied by warming of the troposphere and cooling of the lower stratosphere.

1. Introduction

Meteorological conditions over European Russia (ER) during the unusually long-lasting summer atmospheric blocking episode of 2010 contributed to abnormally high temperatures, lack of rainfall, and the development of wildfires [1]. Heat waves and presence of combustion products (smoke, carbon monoxide, and various hydrocarbons) in the air significantly worsened the ecological conditions, especially in the urbanized regions. Various aspects of manifestations, physical mechanisms, and the effects of this unique natural anomaly were studied in [2–7]. In [2, 3] it was shown that in early August there was an abnormal meridional distribution of TCWV over ER, which was characterized by the WV excess in the northern part of the ER and its deficit in the southern part of the territory. The positive anomalies of WV in the northern part of EE in July 2010 were also documented in [4].

WV is the fourth most abundant of the atmospheric gases and is also the most important greenhouse gas of natural origin [8]. Most of WV is contained in the lower troposphere,

mainly in the tropics [9]. Changes in the phase state of water are accompanied by the release or absorption of large amounts of heat and play an important role in the energy balance and, as a consequence, in the dynamics of the atmosphere. WV in the stratosphere has a significant impact on the photochemical processes in this altitude region [10] and affects the radiation balance of the atmosphere [11]. Due to long life time in the atmosphere (about ten days), WV is carried for long distances by atmospheric currents thus being a tracer of the atmospheric dynamic processes [12, 13].

It is believed that the stability of block's dynamics can be realized due to the feedback mechanisms, involving the interaction between synoptic waves and planetary scale waves, as well as by advective and diabatic processes [14–16]. These processes can force or enhance ridging in the middle troposphere enhancing the vertical motion profile as well. Diabatic processes can enhance blocking events directly [15, 17] or indirectly via advection [14, 16].

The study of the evolution of water vapor in the troposphere and in the stratosphere over northern Europe during

the development of the atmospheric blocking is of great interest, because in the northern Hemisphere the territory of European Russia in the spring and summer, the most prone to the formation of blocking anticyclones, and because of the specific geographical situation of the territory and surrounding water areas. Involvement of WV in the anticyclonic circulation may change sign of the meridional gradient of TCWV and accumulate WV in the north of EE [2–4], where in conditions of a relatively low and warm tropopause it can more easily penetrate into the stratosphere. In this paper, using the satellite and upper air WV observations, the evolution of the horizontal and vertical distribution of WV during the summer 2010 atmospheric blocking over EE, as well as possible impact of WV on the block dynamics, is analyzed.

2. Data and Methods

2.1. Data. The horizontal distribution of WV and its temporal variations during blocking were analyzed on the basis of Moderate Resolution Imaging Spectroradiometer (MODIS) observations. Evolution of the vertical structure of WV was studied on the basis of Microwave Limb Sounder (MLS) and upper air data.

The MODIS instruments (Aqua and Terra satellites) are 36-channel imaging spectroradiometers, measuring reflected solar radiation and emitted surface and atmosphere radiation in the wavelengths 0.4–14.4 μm [18]. The 2330- km scan across the suborbital track allows MODIS to provide daily global coverage of extratropical regions. In this study TCWV, retrieved by the near-infrared (NIR) algorithm (0.86–1.24 μm range), was used [19]. NIR data are more sensitive to boundary-layer WV content than IR data and characterized by relatively small error (5–10%), but restricted by daytime and the surface areas that reflect at these wavelengths. The MOD08_D3/MYD08_D3 (Aqua/Terra) HDF files from MODIS’s collection 5.1 were obtained via LAADS Web server (<http://ladsweb.nascom.nasa.gov/>). Averaged daily and within $1^\circ \times 1^\circ$ grid cells (L3) data [20] were used due to their convenience to study large-scale atmospheric processes than initial (L2) data.

The MLS instrument (Aura platform) is a microwave radiometer/spectrometer, measuring natural thermal emission from the Earth’s limb [21]. MLS retrieves atmospheric WV mixing ratios at heights from the upper troposphere to the upper mesosphere [22]. In this study the data in the range 316.2–46.4 hPa were used. The precision (vertical resolutions) of the water vapor retrievals in the troposphere and stratosphere is estimated to be 35–65% (2–2.5 km), and 6–40% (2.5–3.5 km) respectively. Accompanying temperature retrievals in the pressure range of 261–46.4 hPa were also used. Vertical resolution of temperature profile is about 5 km from 261 hPa to 100 hPa and it improves to 3.6 km at 31.6 hPa. Estimated precision in the lower stratosphere is 0.6 K. The MLS retrieves the vertical profiles every 165 km along the suborbital track, covering the latitudes from 82°S to 82°N on each orbit. The along track horizontal resolution degrades with height and ranges from 210 km to 700 km for water vapor and from 170 km to 220 km for temperature data [23].

TABLE 1: Aerological station, whose data used in this work.

WMO no.	Station	Latitude (N)	Longitude (E)	Elevation (m)
22217	Kandalaksa	67.15°	32.35°	25
22271	Sojna	67.88°	44.13°	16
22820	Petrozavodsk	61.81°	34.26°	110
22845	Kargopol	61.50°	38.93°	126
23205	Narjan-Mar	67.63°	53.03°	12
23804	Syktvykar	61.66°	50.85°	116
23921	Ivdel	60.68°	60.45°	95
26063	St. Petersburg	59.95°	59.95°	78

ML2H2O.003 and ML2T.003 (v.3.3) products were obtained with the help of Giovanni MLS/Aura online visualization and analysis system (<http://disc.sci.gsfc.nasa.gov/giovanni>) [24]. The data have been filtered according to the recommended screening values as given in the MLS data quality document.

WV and temperature evolution in the troposphere and lower stratosphere were also studied on the basis of radiosonde data from eight aerological stations (Table 1). The profiles were taken from the archive of the upper air observations, created and maintained at the University of Wyoming (<http://www.weather.uwyo.edu/>). The humidity sensors used in the Russian radiosondes are not certificated at temperatures below -40°C . These sensors significantly overestimate the relative humidity of air in the lower stratosphere as compared with those used in the Vaisala RS-92 radiosonde. Because of that, in this study on the basis of radiosonde measurements only qualitative evaluation of WV changes in the stratosphere will be presented.

The atmospheric dynamics during blocking episode were determined by using National Centers for Environmental Prediction/National Center for Atmospheric Research (NCEP/NCAR) reanalysis data [25]. These data were provided on the 2.5° by 2.5° latitude-longitude grids available on 17 mandatory levels from 1000 hPa to 10 hPa at (<http://www.esrl.noaa.gov/psd/data/reanalysis/>). Daily geopotential height and vertical velocity (ω) data were used in this study. Vertical velocity data were provided on 12 levels up to 100 hPa.

2.2. Methods. The blocking definition used here is described in [4] and references therein. Briefly, this definition is a combination of a subjective blocking definition that uses split flow as the main criterion, and an objective “zonal index” criterion. The zonal index is calculated by taking the height at 40°N and subtracting the height at 60°N along a longitude line at 500 hPa, which is proportional to the geostrophic wind. Where this value is less than zero over 30 degrees longitude and for five or more days indicates blocking. The blocking criterion used here includes (i) the appearance of split flow for a minimum of five days; (ii) a negative or small positive zonal index (less than 50 units [6]), must be identified on a time-longitude or Hovmöller diagram; (iii) conditions (i) and (ii) satisfied for 24 h after (before) onset (termination); (iv) the blocking event should be poleward of 35°N during its lifetime, and the ridge should have an amplitude of greater

TABLE 2: Blocking events occurring during the summer of 2010 and identified by [4].

Event	Onset	Termination	Duration (days)	Formation (longitude)
1	22 June	June 28	6	50°E
2	4 July	July 30	26	20°E
3	31 July	August 16	15.5	45°E

than 5° latitude; and (v) blocking onset is determined to occur when condition (iv) and either conditions (i) or (ii) are satisfied, while (vi) termination is designated at the time the event fails condition (v) for a 24 h period or longer. This procedure is used to detect the blocking events at 500 hPa and defines the blocking duration using these start and end dates. The blocking events studied here are listed in Table 2. In this analysis, the onset (termination) period is defined as the three-day period before (following) block onset defined above, while intensification (decay) is represented by a general increase (decrease) in center point heights. Maintenance is generally represented by periods where the center point time tendency is close to zero.

3. Results

3.1. Space-Time Evolution. In accordance with the results of the performed diagnostics the episodes of atmospheric blocking took place over EE from June 22 to August 16 2010 (Table 2). Figure 1 represents the evolution of TCWV before, during, and after a blocking situation. The figure shows the differences between the spatial distributions of TCWV contents averaged over 10-day periods and the spatial distribution of the average TCWV contents in the period 10–19 June, that is, in the period immediately preceding the block. Such an approach eliminates the small-scale anomalies and irregularities, but highlights the dominant features of the evolution of TCWV associated with the evolution of the block. For each period a corresponding average spatial distribution of the 700 hPa height is also shown.

In the period 12–21 June, the spatial distribution of TCWV over Europe was still close to the climatological distribution. By late June the ridge, associated with the Azores High, extended from Azores islands to the Norwegian Sea and promoted the inflow of cool dry Arctic air into the north of Europe. Subsequent formation of a cyclone to the south from Iceland (June 24–July 3) shifted the ridge to the east and led to the inflow of moist Atlantic air into this region. The high humidity of the incoming air could be due, at least in part, to the record positive anomalies of the sea surface temperatures (SSTs) observed in the first half of 2010 in the Tropical Atlantic (10°–20°N; 20°–85°W) [26]. The anomalous SSTs contributed to the evaporation of water.

In early July, a strengthening of the Azores High and the deepening of the Icelandic Low increased the inflow of the WV into northern Europe but the subsequent mid-July weakening of the Azores High and filling of the Icelandic Low weakened the inflow of Atlantic air. The concurrent

formation over ER of the blocking pattern known as a Rex block (4–13 July–18–27 July) contributed to the meridional transport of WV and thereby increased regional atmospheric moisture content. In late July, the Rex block over ER transformed into omega block, which is evident in the distribution of 700 hPa heights up to 7–16 August period. In early August, another enhancement of the Azores High and the formation of a cyclone southeast from Iceland renewed the increased inflow of moist Atlantic air in Europe, while the concomitant strengthening of the omega block had led to the strong winds in the northern part of ER. These winds moved the moist air along the northern periphery of the anticyclone, predominantly in the zonal direction far to the east in Western and Central Siberia.

Early August was the apex of the development of the TCWV abundance over the north of EE associated with the blocking episode. The maximum increase of TCWV (in comparison with the period before blocking) was observed over the territory restricted by the coordinates 60°–70°N and 30°–60°E. In this region the average TCWV content between the periods 10–19 June and 28 July–6 August had increased from 1.02 cm to 2.95 cm, that is, in fact nearly tripled. In the resolution 1° × 1° the TCWV changes were even greater and reached the factor of 3.4 (64°–65°N; 54°–55°E). The largest decrease of TCWV in this period occurred in the south of ER (over the North Caucasus).

Figure 2(a) shows the difference between the TCWV distribution in the first ten days of August in 2010 and that in the period 2000–2009. The climatological distribution of TCWV over EE in the summer season is close to zonal and characterized by the mean meridional gradient of –0.4 mm/100 km (TCWV decreases from south to north). It is seen that the distribution of TCWV in early August 2010 was anomalous, with the WV excess in the north of EE and its deficit in the south of EE. Between 40 and 45°E the mean meridional gradient of TCWV changed sign and reached +1 mm/100 km [2].

A comparison of the TCWV anomalies and the 700 hPa horizontal wind data (black arrows) evidences that the main features of the spatial distribution of TCWV in this period were determined by atmospheric dynamics associated with an omega block (Figure 2(b)), which compelled the air to move north along the western periphery of the anticyclone and return over the Ural Mountains. With the advance to the north the velocity of the air flow increased. The maximum 10-day average wind speed in the region was reported in the northern part of ER and reached 16 m/s at the 700 hPa level, while the center of block was characterized by light winds. The anomalies of 700 hPa height (ΔH_{700}) in the center of the block during 1–10 August (hereinafter, unless specifically stated, all dates are 2010) exceeded 160 g.p.m.

The arc-shaped spatial distribution of the positive anomalies of TWVC in Figure 2(a) reflects the advection of warm, moist, maritime air from the eastern Mediterranean and the Black Sea to the northern part of EE. The advection of warm, moist air in the lower troposphere would likely enhance 500 hPa ridging in the blocking region [27, 28]. Localization of the maximum of TCWV anomalies over the north of ER can be explained as the combined effect of the WV advection

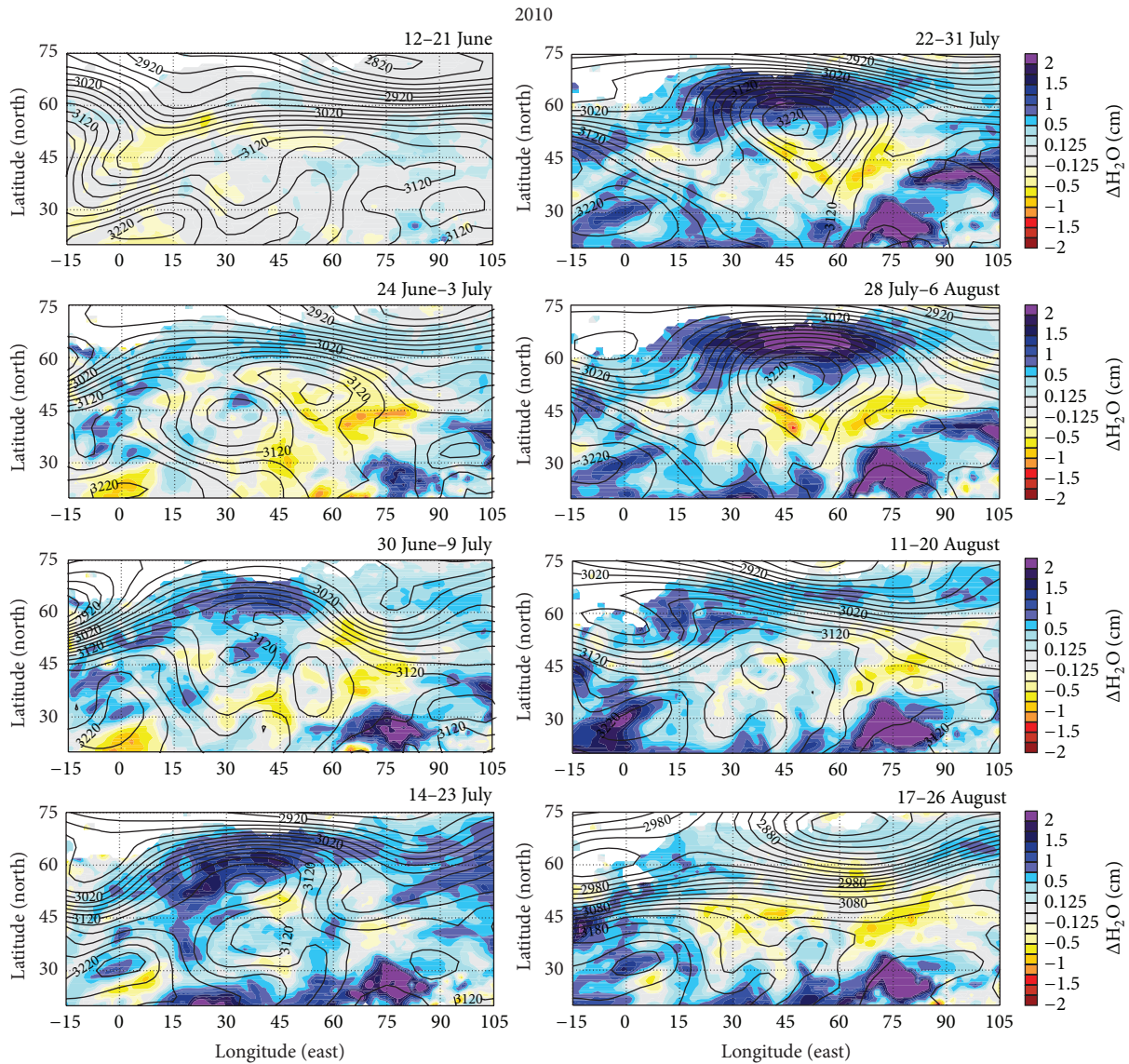


FIGURE 1: Differences between TCWV content averaged over 10-day periods (shown above each plot) and average TCWV content in the period 10–19 August 2010. Isolines are average 700 hPa heights for the same periods.

and an intensification of evaporation from the numerous water objects (rivers, lakes, and swamps), which are characteristic for this territory, due to high temperature and strengthening of wind. The high temperature of air also contributed to trapping more WV in the air. The influx of latent heat in the block area could contribute to the energy supply of the blocking anticyclone and prolong its existence. Lower tropospheric latent heat was demonstrated to enhance blocking [15] by forcing height rises in the midtroposphere. The meridional flow of moist air to the north of Eastern Europe originated in tropical and subtropical areas, where the tropopause is located at altitudes which are in middle and high latitudes that are already in the stratosphere. When moving from north to south, moist air from the low-latitude upper troposphere through the tropopause breaks could enter the lower stratosphere in the mid- and high-latitudes.

Figure 2(c) shows the anomalies of the vertical wind velocity at 500 hPa level. It is seen that, along the western and northern peripheries of the anticyclone, the ascending motions of air existed. Analysis of data at other tropospheric levels showed that these motions covered the entire troposphere. The ascending motions of air could contribute to the increase of the TCWV content because they promoted water vapor outflow from the surface up, while the high temperature helped to maintain large amounts of moisture in the air.

In the second ten days of August a sharp weakening of the omega block over ER and the formation of a trough over the North Atlantic and deep cyclone over the Kara Sea led to the inflow of dry cool Arctic air into Northern and Eastern Europe (Figure 1). Interestingly, weakening and destruction of the blocking anticyclone over ER were accompanied by the

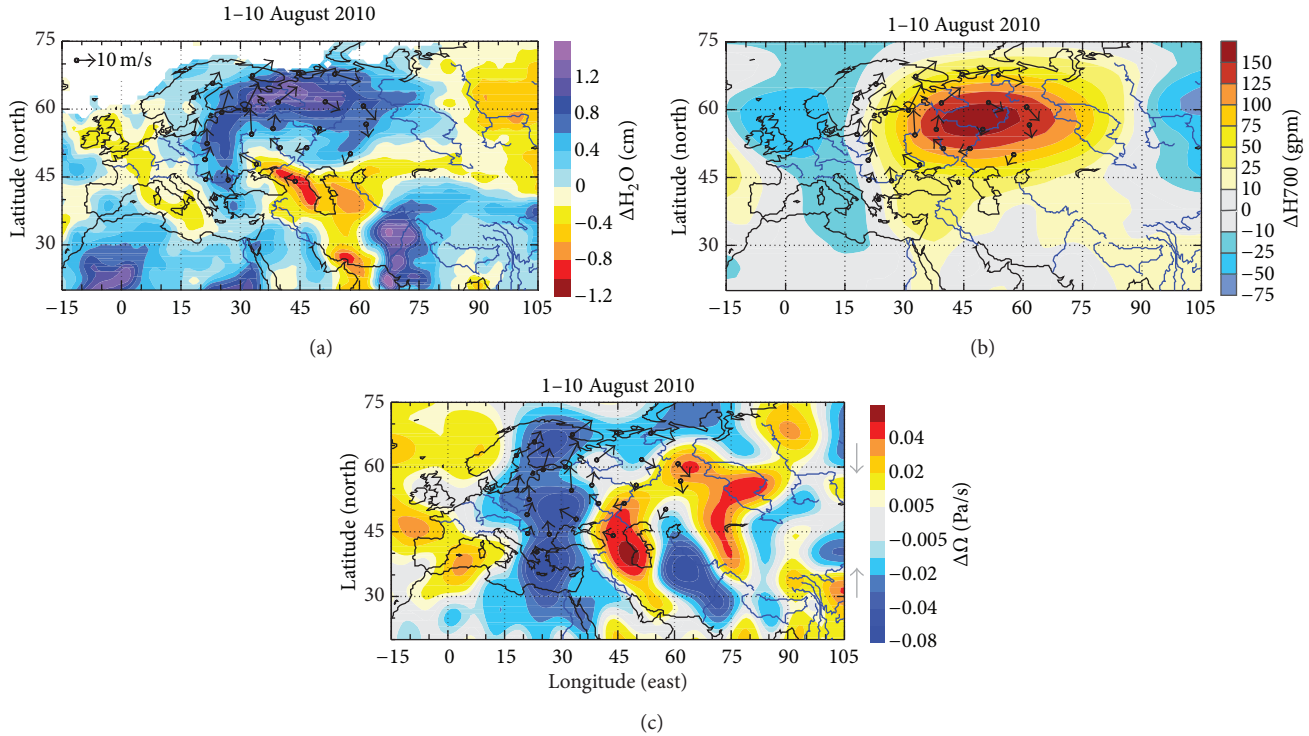


FIGURE 2: Differences between averages in the period 1–10 August 2010 and averages in the period 1–10 August 2000–2009 for TCWV (a), 700 hPa height (b), and vertical velocity (c). Arrows represent the mean wind vectors at 700 hPa (taken from [3]).

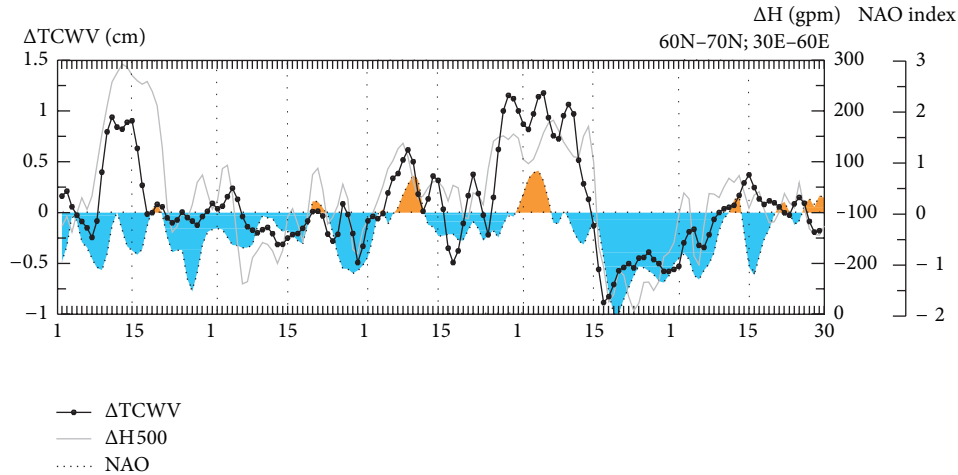
weakening and, ultimately, the disappearance of the Azores High.

3.2. Connection with the North Atlantic Oscillation. Figures 1 and 2 evidence that the changes of WV over EE in the summer of 2010 were closely related to the atmospheric blocking dynamics. Figure 3 shows the time-series of the daily anomalies of TCWV and H500 in the regions 60°–70°N; 30°–60°E and 40–50°N; 30°–60°E, where the changes of WV associated with the block reached maxima but were characterized by the opposite signs. Daily anomalies were calculated as the difference between the area-averaged values of TCWV in 2010 and the long-term area-averaged values of TCWV calculated for the same days in the period 2000–2009. It is seen that in the northern part of ER the evolution of TCWV and the evolution of H500 were characterized by a notable resemblance. The correlation coefficient between TCWV and H500 variations during May–September was 0.72 (95% CI: 0.63, 0.79), while for June–August it increased to 0.78 (0.68–0.85). In the southern part of ER the evolution of the TCWV was not associated with the evolution of H500 (Figure 3(b)). In both periods the correlation coefficients between the TCWV and H500 variations were close to zero. Variations of the H500 anomalies in the northern and southern ER were characterized by a weak positive correlation (0.37) between each other, while the corresponding TCWV variations revealed a weak negative correlation (–0.26). Analysis of the data for other years showed that for the north of the territory a positive correlation between TCWV and H500 anomalies is fairly typical. Because H500

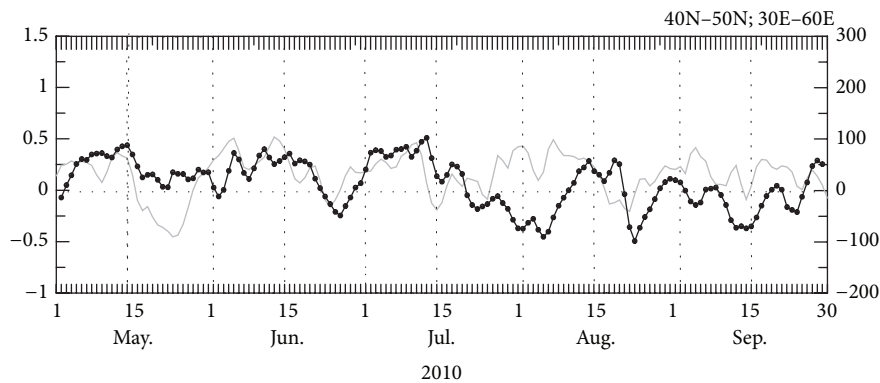
depends on the mean air temperature below 500 hPa level, such a correlation is due to the ability of air to hold more moisture at higher temperatures.

An important factor regulating the westerly transfer of air masses over Europe is the North Atlantic Oscillation (NAO). Figure 3(a) also shows the values of normalized daily NAO index from May to September (<http://www.cpc.ncep.noaa.gov/>). A comparison of TCWV and H500 anomalies with the NAO index evidences that the evolution of TCWV over EE during atmospheric blocking was affected by both local and remote atmospheric processes. The correlation coefficient between the daily regional TCWV anomalies in the northern part of ER and the daily NAO index for May–September was 0.50 (0.37, 0.61) and increased to 0.66 (0.51–0.75) during June–August. Analysis of the data for other years showed that the magnitude and even the sign of the correlation between the WV anomalies and NAO index changed from year to year (Figure 4). In the period 2000–2004 the changes of the TCWV were weakly dependent on the pressure changes in the North Atlantic. In 2005 there was a significant negative correlation between the TCWV and NAO. From 2005 till 2010 there was a trend to a change in the sign and increase in the absolute values of correlation coefficients. The maximum positive correlation between the TCWV anomalies and the NAO index has been achieved in 2010. In the consequent two years, this relationship has weakened (2011) and then changed sign (2012).

3.3. Height-Time Evolution. The TCWV is the integral characteristic of water vapor content in the atmospheric column.



(a)



(b)

FIGURE 3: Daily anomalies of TCWV and 500 hPa height averaged over the territories restricted by the coordinates 60° – 70° N; 30° – 60° E (a) and 40° – 50° N; 30° – 60° E (b). For each day the anomalies were calculated as difference between daily average in 2010 and average for this day in 2000–2009. In (a) the daily normalized NAO index is also depicted.

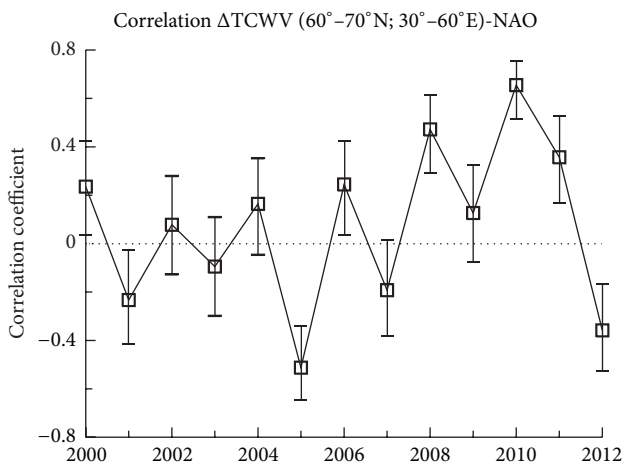


FIGURE 4: Correlation coefficients between the daily TCWV anomalies averaged over the territory restricted by the coordinates 60° – 70° N; 30° – 60° E and the daily normalized NAO index in June–August calculated for each year in the period 2000–2012. Vertical bars denote $\pm 95\%$ confidence intervals.

Since the bulk of water vapor resides in the lower 1–2 km layer of the atmosphere, the evolution of TCWV reflects the dynamic processes occurring mainly in the lower troposphere. However, the summer 2010 blocking anticyclone over the ER revealed itself not only in the troposphere but also in the stratosphere. During the first ten days of August, closed isohypses could be traced at 50 hPa pressure level (not shown). Therefore, the water vapor changes caused by this blocking episode could be manifested in the wide range of atmospheric heights.

3.3.1. Upper Air Data. Figures 5(a) and 5(b) show the anomalies of WV and temperature in the troposphere and lower stratosphere during May–September, calculated using data from eight upper air stations located in the north of ER (Table 1). For each day, the anomaly was calculated as the difference between the daily mean value and 3-month (91 days) moving average. It is seen from the figures that as early as during the first blocking event (Table 2), there were two short-term increases of WV in the troposphere, accompanied by warming of air, while between the first and the second

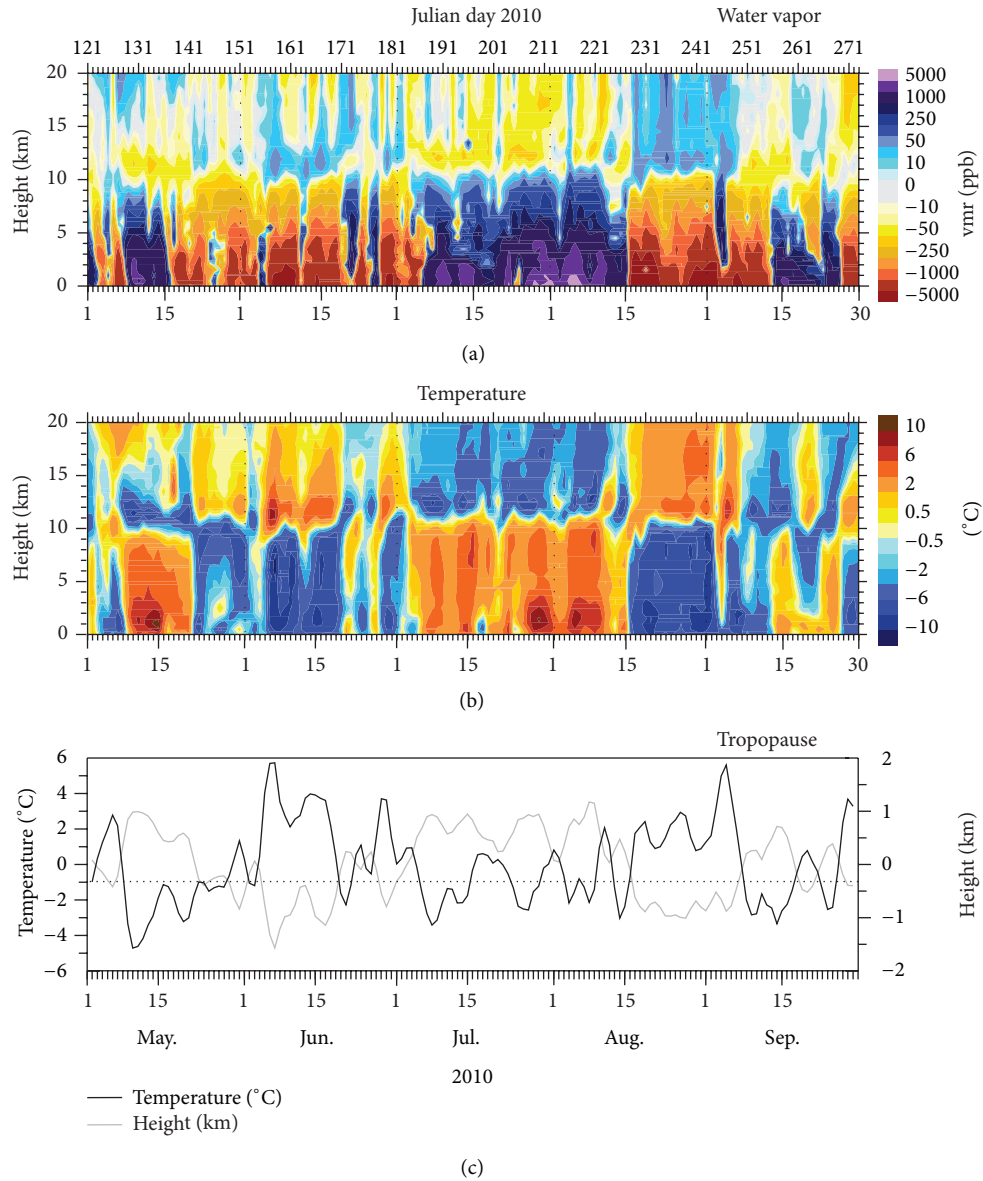


FIGURE 5: The time-height section of (a) water vapor anomalies in May–September 2010, calculated using radiosonde data from 8 upper air stations located in the north of ER (see Table 1), (b) the same, but for temperature. (c) The anomalies of the tropopause height (grey line) and temperature (black line).

blocking events the deficit of water vapor and the cooling in the troposphere occurred. The connection of these changes with block dynamics however are less evident because during the whole period under review the temperature anomalies in the troposphere and stratosphere positively correlated with corresponding WV anomalies. The main features of the evolution of WV and temperature in the summer of 2010 manifested themselves during the second and third blocking events and also after termination of the block in the second half of August. Since the beginning of July to mid-August there was a positive anomaly (excess) of WV in the troposphere and a negative anomaly (deficit) of WV

in the stratosphere (Figure 5(a)). Changing the signs of the tropospheric and stratospheric WV anomalies coincides with the end of the block (Table 2). Humidification of the troposphere and dehumidification of the lower stratosphere during the second and third blocking events were accompanied by warming of the troposphere and cooling of the lower stratosphere. Using height tendency dynamics [27, 28], these would both enhance blocking. The time-height variations of WV in the troposphere over the north of EE agree well with the changes in the spatial distribution of TCWV (cf. Figures 5(a) and 1). Quantitative estimations of tropospheric WV changes can be found in Table 3, which contains the average

TABLE 3: Water vapor anomalies in the surface layer (0 km) and at the altitudes 3 km and 8 km (ppm) as well as the anomalies of tropopause height (H trop (km)) and temperature (T trop ($^{\circ}$ C)) before (P1), during (P2), and after (P3) blocking events of the summer 2010 and their differences obtained using upper air data (Table 1). The percentage differences in relation to the local yearly mean values are shown in parentheses. Last column represent a probability (P value) that the medians of three groups of the anomalies are from the same population, calculated using the Kruskal-Wallis test.

Altitude (km)	P1: 7–21 June	P2: 22 June–16 August	P3: 17–31 August	P1–P2		P3–P2		P value
8	–103	122	–193	225	(101)	–315	(–142)	$8 \cdot 10^{-9}$
3	–1045	840	–1540	1885	(65)	–2380	(–82)	$5 \cdot 10^{-9}$
0	–2092	1839	–3268	3931	(59)	–5107	(–76)	$7 \cdot 10^{-11}$
H trop	–0.8	0.4	–0.9	1.2	(12)	–1.3	(13)	$4 \cdot 10^{-11}$
T trop	2.4	–0.6	1.8	–3	(–5)	2.4	(4)	$3 \cdot 10^{-6}$

values of WV anomalies in the surface layer and at the heights 3 km and 8 km in the two weeks preceding the block, in the blocking periods, and in the two weeks following the block as well as the differences in these values. The estimates of the significance of differences between the median values of the anomalies in these time intervals, calculated on the basis of the Kruskal-Wallis test, are also presented. The test results showed that the differences between the WV anomalies obtained in these periods are highly statistically significant. The data in Table 3 also evidence that in relative units the maximum increase of WV during the block was observed in the upper troposphere. This fact shows the crucial role of advective processes in the formation of the positive anomaly of TCWV over the north of EE in the blocking period.

The time-height structure of the temperature variations in May–September revealed the patterns of “atmospheric dipoles.” It is seen that the positive anomalies in the troposphere are accompanied by the negative anomalies in the stratosphere and vice versa (Figure 5(b)). The changes of temperature in the upper troposphere and lower stratosphere (UTLS) affect the tropopause position and temperature. Figure 5(c) shows that the anomalies of the tropopause height and the anomalies of the tropopause temperature were in the antiphase. The correlation coefficient between them in May–September amounted to -0.82 (-0.87 , -0.76). Antiphase variations in tropopause height and temperature indicate that an important role in the tropopause formation in this period played dynamic factors, in particular adiabatic processes, associated with the vertical motions of air. The correlation analysis showed that WV vapor content more (less) strongly correlated with the tropopause height (tropopause temperature), respectively. In summer the strongest correlation with the tropopause characteristics revealed the water vapor content in the upper troposphere. In June–August the correlation between the tropopause height and WV content at 8 km reached the value 0.85 (0.78 , 0.90), whereas the correlation between the tropopause temperature and WV content at the same height amounted to -0.62 (-0.73 , -0.48). Variations in the tropopause height during the block ranged between 10.1 km and 12.6 km, with the mean value of 11.4 km.

The analysis of the upper air data reveals in general fairly agreed changes in water vapor, temperature, and tropopause characteristics. Comparison of Figure 5(a) with Figure 5(c) shows that increasing the height of the tropopause (and

decreasing of the tropopause temperature) is accompanied by increasing in tropospheric water vapor and some decrease in water vapor in the stratosphere. On the contrary, decreasing the height of the tropopause (and increasing the tropopause temperature) was accompanied by a decreasing of tropospheric water vapor content and by slight increasing in water vapor in the region above the tropopause. Adjusting the freezing of water vapor, the tropopause regulates the water vapor flux from the troposphere to the stratosphere. Cold tropopause hampers the penetration of water vapor from the troposphere to the stratosphere, locking it, thus, in the troposphere (where high temperatures, which were observed in the summer of 2010, helped retain large amounts of moisture in the air). It is seen from Figure 5(c) that with the destruction of the block there was a sharp decrease in the tropopause height (by 2 km within 10 days) accompanied by the increase in tropopause temperature. The increase in stratospheric WV after the block could be at least in part caused by the injection of WV from the troposphere to the stratosphere due abrupt lowering of the tropopause given the water vapor abundance in the upper troposphere.

3.3.2. MLS Data. Figures 6(a) and 6(b) show the WV and temperature anomalies between the pressure levels 316 and 46.6 hPa, obtained on the basis of MLS data (the lower and the upper levels correspond to the heights of about 9 km and 20 km). For each of the days, the daily mean WV profile was calculated on the basis of seven profiles, which were nearest to the point with the coordinates 65° N and 50° E, but not beyond the area bounded by coordinates 60° – 70° N and 40° – 60° E. In the same manner the daily mean temperature profiles were calculated. As in case of radiosonde data processing, the daily anomalies were calculated as the differences between the daily mean values and the mean values obtained using 3-month moving average operator.

In the upper troposphere, the evolution of WV in May–September obtained from MLS observations is consistent with the evolution of WV obtained from upper air observations (cf. Figures 5(a) and 6(a)). Before and after the block the upper troposphere was dominated by negative WV anomalies, while during the block the strong positive WV anomalies prevailed in the upper troposphere. The change of the prolonged positive WV anomaly associated with the block to the negative one almost exactly coincided with

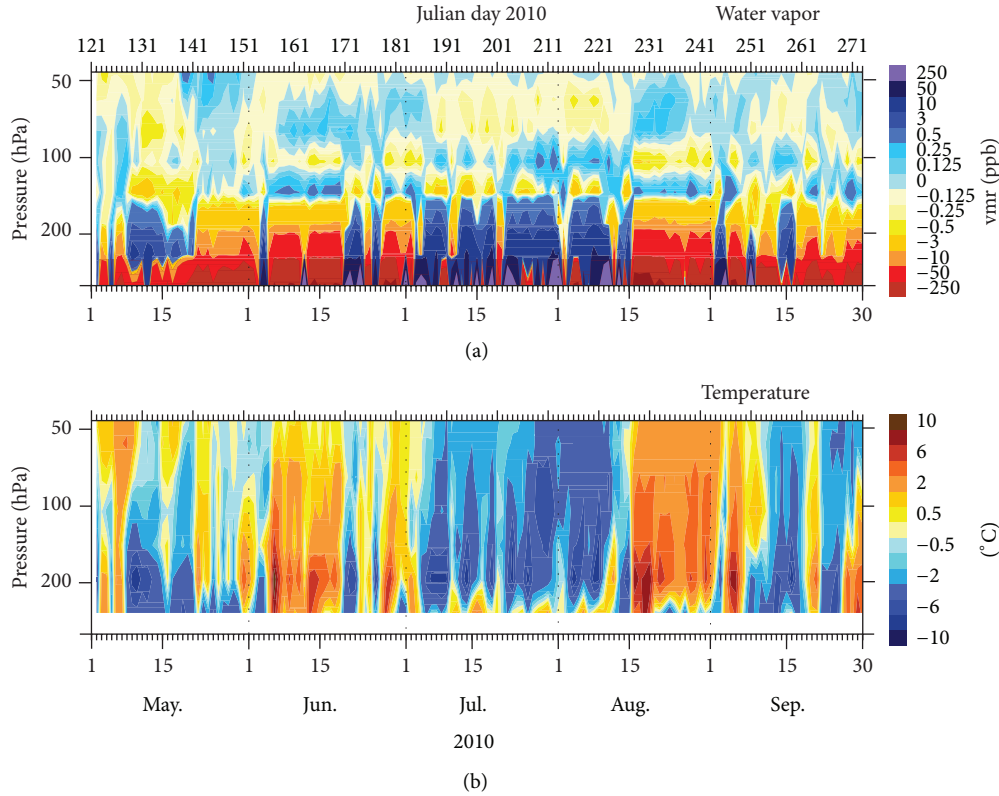


FIGURE 6: The time-height section of (a) water vapor anomalies in May–September 2010, calculated using MLS data centered at 65°N and 50°E, (b) the same, but for temperature.

TABLE 4: Water vapor anomalies in the UTLS region (ppm) according to the MLS data, centered at 65°N, 50°E. The rest as in Table 3.

Level (hPa)	P1: 7–21 June	P2: 22 June–16 August	P3: 17–31 August	P1–P2		P3–P2		<i>P</i> value
46	-0.154	0.013	-0.048	0.167	(3)	-0.061	(1)	$2 \cdot 10^{-5}$
56	-0.044	-0.046	0.081	-0.002	(0)	0.127	(3)	0.006
68	0.025	-0.129	0.326	-0.154	(-3)	0.455	(10)	$4 \cdot 10^{-9}$
83	0.258	-0.44	0.146	-0.698	(-16)	0.586	(13)	$1 \cdot 10^{-8}$
100	-0.175	0.178	-0.390	0.353	(8)	-0.568	(-12)	$5 \cdot 10^{-7}$
121	-0.204	0.073	-0.176	0.277	(6)	-0.249	(-5)	0.004
147	0.933	-0.365	0.924	-1.30	(-29)	1.30	(29)	$7 \cdot 10^{-8}$
178	-1.42	1.32	-2.26	2.74	(51)	-3.57	(-67)	$8 \cdot 10^{-9}$
215	-9.30	6.68	-11.81	16.0	(179)	-18.6	(-208)	$7 \cdot 10^{-9}$
261	-32.1	25.2	-43.7	57.3	(165)	-68.9	(-198)	$4 \cdot 10^{-9}$
316	-104	160	-221	264	(148)	-381	(-214)	$3 \cdot 10^{-5}$

the end of the blocking events (Table 2). Quantitative estimates of WV changes in the UTLS region before, during, and after the block obtained using MLS data can be found in Table 4. The data in the table indicate that the absolute values and the changes of the WV contents in the upper troposphere in these periods according to both the platforms (satellite and balloon) were close to each other.

In the stratosphere the MLS instrument revealed more complex pattern of the WV changes. During the block the WV decrease occurred at the levels 147, 82, 68, and 56 hPa, while the WV increase was observed at the levels 121 and 100 hPa. Interestingly, after termination of the block the WV

vapor decrease was on the contrary observed at 121 and 100 hPa, while the increase occurred at 147, 82, 68, and 56 hPa. The time-height structures of the anomalies of temperature and WV obtained using MLS data do not seem to be quite consistent with each other (as compared with those obtained using upper air data). So, quite abrupt changes in water vapor between the levels 178 and 147 hPa are not traced in temperature. It is also difficult to assume that the presence of the physical mechanisms causes opposite tendencies of changes of water vapor in a narrow altitude region. As noted above the water vapor sensors used in Russian radiosondes are not quite reliable in the stratosphere. On the other hand,

it is known that MLS overestimates water vapor content in the wettest conditions [29] and is dry biased at low levels [22]. Detailed analysis of the reasons for the discrepancies in the water vapor evolution above the tropopause, which have been noticed in the results of the analyses of the upper air and MLS data is of great interest, however, is beyond the scope of this paper. Therefore, here we restrict ourselves to pointing out the existence of such differences.

The changes in temperature in the pressure range 261–46.6 hPa, obtained using MLS data (Figure 6(b)), agree well (qualitatively and quantitatively) with the temperature changes at heights 10–20 km, obtained using radiosonde data (cf. Figures 5(b) and 6(b)). In the two-week periods before and after the block the lower stratosphere was anomalously warm, while during the block the lower stratosphere was anomalously cold. Quasiperiodic antiphase temperature changes in the troposphere and lower stratosphere (Figures 5(b) and 6(b)) can be explained by the meridional motions of air occurring synchronously in a wide range of heights in the troposphere and stratosphere. The cause of such motions can be traveling planetary waves (it is worthy to remind that over the region under review the meridional gradients of temperature have opposite signs in the troposphere and stratosphere). During the block due to converting traveling waves to stationary waves a key role in the changes of water vapor (and temperature) in the north of EE probably played the advection embracing the troposphere and lower stratosphere, and thus synchronously transporting the air in the wide range of heights from the tropics to the high latitudes.

4. Conclusion

On the basis of satellite (MODIS and MLS instruments), aerological, and NCAR/NCEP reanalysis data, an analysis of the spatial and temporal variability of the water vapor plume over EE during the unusually long episode of the summer 2010 atmospheric blocking was carried out.

The obtained results show that the development of blocking was accompanied by the development of a positive anomaly of the TCWV in the northern part of EE, which reached its maximum in the period 28 July–6 August. The mean TCWV content averaged over the region 60°–70°N, 30°–60°E in this period amounted to 2.95 cm and almost tripled with respect to that before blocking. The gridded (1° × 1°) TCWV content reached the value 3.35 cm in this region (an increase 3.3 times). The surplus of TCWV was mainly conditioned by the advection of water vapor. The peculiarities of atmospheric circulation over EE and the northern Atlantic promoted the transfer of warm and moist air from the Atlantic Ocean and the Mediterranean Sea into the north of EE. The strengthening of wind in the north of EE and high temperature contributed to increased evaporation from the surface enriched with water, while high temperature also helped to retain large amounts of water vapor in the air. The influx of latent heat into the block area could contribute in energy supply of the blocking anticyclone and thus prolong the existence of the block. The positive anomaly of TCWV in the north of EE in the blocking conditions is apparently

a regional phenomenon due to geographic location of the region and atmospheric dynamics characteristic for the summer block. The changes in TWVC in the north of EE in the summer periods of 2000–2012 were characterized by varying degrees of connectedness with the North Atlantic oscillation. The analysis showed that the maximum positive correlation between the TWVC anomalies and the NAO index in these periods (0.66) was achieved exactly in the summer of 2010.

The changes in water vapor and temperature associated with the blocking episode of the summer 2010 manifested themselves in the troposphere and in the lower stratosphere. The increase in tropospheric content of water vapor during the block is confirmed by the results of the analyses of the upper air data and MLS data. In the upper troposphere there is qualitative and quantitative agreement between estimates of the water vapor changes obtained using data from both platforms. The calculation results indicate that the strongest relative increase of water vapor during the block occurred just in this region. The situation in the stratosphere is not so clear. According to radiosonde data above the mean tropopause position (11.4 km) the negative anomalies of water vapor prevailed. The changes in water vapor associated with the block positively correlated with the changes in temperature: the excess of water vapor in the troposphere was accompanied by warming of the troposphere, while the deficit of water vapor in the stratosphere was accompanied by cooling of the stratosphere. According to MLS observations the mean content of water vapor between the pressure levels 147 and 47 hPa (~13.5–20 km) has also decreased during the block, whereas the local water vapor mixing ratios at 121 hPa and 100 hPa levels have increased in the blocking period.

In a whole, the period of the atmospheric blocking was characterized by more higher and more colder tropopause as compared with the periods which precede and follows the block. The changes in water vapor and temperature revealed clear correlation with the changes in tropopause characteristics. The highest correlation ($r = 0.85$) was found between the height of the tropopause and the water vapor content in the upper troposphere.

Conflict of Interests

The authors declare that there is no conflict of interests regarding the publication of this paper.

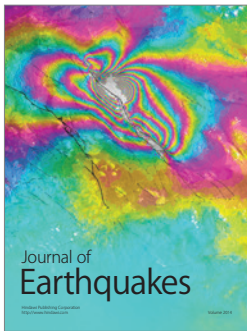
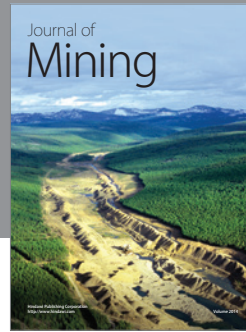
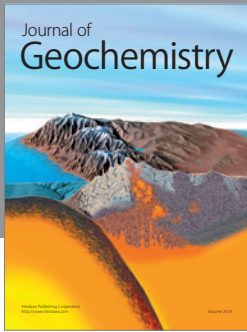
Acknowledgments

This work was supported by the Russian Foundation for Basic Research (Grants 11-05-00704_a, 12-05-91057-CNRS_a, 13-05-41432_a, and 14-05-00639_a), by the Grant of the RF President NSh-3894.2014.5, and by programs of the Russian Academy of Sciences.

References

- [1] I. I. Mokhov, "Specific features of the 2010 summer heat formation in the European territory of Russia in the context of general climate changes and climate anomalies," *Izvestiya, Atmospheric and Oceanic Physics*, vol. 47, no. 6, pp. 653–660, 2011.

- [2] S. A. Sitnov and I. I. Mokhov, "Peculiarities of water vapor distribution in the atmosphere over the European part of Russia in summer 2010," *Doklady Earth Sciences*, vol. 448, part 1, pp. 86–91, 2013.
- [3] S. A. Sitnov and I. I. Mokhov, "Water-vapor content in the atmosphere over European Russia during the summer 2010 fires," *Izvestiya, Atmospheric and Oceanic Physics*, vol. 49, no. 4, pp. 380–394, 2013.
- [4] A. R. Lupo, I. I. Mokhov, M. G. Akperov, A. V. Chernokulsky, and H. Athar, "A dynamic analysis of the role of the planetary- and synoptic-scale in the summer of 2010 blocking episodes over the European part of Russia," *Advances in Meteorology*, vol. 2012, Article ID 584257, 11 pages, 2012.
- [5] A. Schneider, S. Schubert, P. Vargin et al., "Large scale flow and the long-lasting blocking high over Russia," *Monthly Weather Review*, vol. 140, no. 9, pp. 2967–2981, 2012.
- [6] M. Matsueda, "Predictability of Euro-Russian blocking in summer of 2010," *Geophysical Research Letters*, vol. 38, no. 6, Article ID L06801, 2011.
- [7] C.-C. Hong, H.-H. Hsu, N.-H. Lin, and H. Chiu, "Roles of European blocking and tropical-extratropical interaction in the 2010 Pakistan flooding," *Geophysical Research Letters*, vol. 38, no. 13, Article ID L13806, 6 pages, 2011.
- [8] A. E. Dessler and S. C. Sherwood, "Atmospheric science: a matter of humidity," *Science*, vol. 323, no. 5917, pp. 1020–1021, 2009.
- [9] A. E. Dessler and K. Minschwaner, "An analysis of the regulation of tropical tropospheric water vapor," *Journal of Geophysical Research D*, vol. 112, no. 10, Article ID D10120, 2007.
- [10] J. G. Anderson, D. M. Wilmoth, J. B. Smith, and D. S. Sayres, "UV dosage levels in summer: increased risk of ozone loss from convectively injected water vapor," *Science*, vol. 337, pp. 835–839, 2012.
- [11] M. Riese, F. Ploeger, A. Rap et al., "Impact of uncertainties in atmospheric mixing on simulated UTLS composition and related radiative effects," *Journal of Geophysical Research*, vol. 117, no. 16, Article ID D16305, 2013.
- [12] A. Werner, C. M. Volk, E. V. Ivanova et al., "Quantifying transport into the Arctic lowermost stratosphere," *Atmospheric Chemistry and Physics*, vol. 10, no. 23, pp. 11623–11639, 2010.
- [13] F. Ploeger, G. Günter, P. Konopka et al., "Horizontal water vapor transport in the lower stratosphere from subtropics to high latitudes during boreal summer," *Journal of Geophysical Research*, vol. 118, no. 14, pp. 8111–8127, 2013.
- [14] J. A. Renwick and M. J. Revell, "Blocking over the South Pacific and Rossby wave propagation," *Monthly Weather Review*, vol. 127, no. 10, pp. 2233–2247, 1999.
- [15] A. R. Lupo and L. F. Bosart, "An analysis of a relatively rare case of continental blocking," *Quarterly Journal of the Royal Meteorological Society*, vol. 125, no. 553, pp. 107–138, 1999.
- [16] F. J. Sáez de Adana and S. J. Colucci, "Southern Hemisphere blocking onsets associated with upper-tropospheric divergence anomalies," *Journal of the Atmospheric Sciences*, vol. 62, no. 5, pp. 1614–1625, 2005.
- [17] D. E. Tilly, A. R. Lupo, C. J. Melick, and P. S. Market, "Calculated height tendencies in two southern hemisphere blocking and cyclone events: the contribution of diabatic heating to block intensification," *Monthly Weather Review*, vol. 136, no. 9, pp. 3568–3578, 2008.
- [18] V. V. Salomonson, W. L. Barnes, P. W. Maymon, H. E. Montgomery, and H. Ostrow, "MODIS: advanced facility instrument for studies of the earth as a system," *IEEE Transactions on Geoscience and Remote Sensing*, vol. 27, no. 2, pp. 145–153, 1992.
- [19] B.-C. Gao and Y. J. Kaufman, "Water vapor retrievals using Moderate Resolution Imaging Spectroradiometer (MODIS) near-infrared channels," *Journal of Geophysical Research D*, vol. 108, no. 13, pp. 1–10, 2003.
- [20] P. A. Hubanks, M. D. King, S. Platnick, and R. Pincus, "MODIS atmosphere L3 gridded product," Algorithm Theoretical Basis Document ATBD-MOD-30, 2008.
- [21] J. W. Waters, L. Froidevaux, R. S. Harwood et al., "The Earth Observing System Microwave Limb Sounder (EOS MLS) on the aura satellite," *IEEE Transactions on Geoscience and Remote Sensing*, vol. 44, no. 5, pp. 1075–1092, 2006.
- [22] N. J. Livesey, W. G. Read, L. Froidevaux et al., "EOS MLS version 3.3 level 2 data quality and description document," JPL D-33509, 2011.
- [23] L. Froidevaux, N. J. Livesey, W. G. Read et al., "Early validation analyses of atmospheric profiles from EOS MLS on the Aura satellite," *IEEE Transactions on Geoscience and Remote Sensing*, vol. 44, no. 5, pp. 1106–1121, 2006.
- [24] J. G. Acker and G. Leptoukh, "Online analysis enhances use of NASA earth science data," *Eos, Transactions American Geophysical Union*, vol. 88, no. 2, pp. 14–17, 2007.
- [25] E. Kalnay, M. Kanamitsu, R. Kistler et al., "The NCEP/NCAR 40-year reanalysis project," *Bulletin of the American Meteorological Society*, vol. 77, no. 3, pp. 437–471, 1996.
- [26] Z.-Z. Hu, A. Kumar, B. Huang, Y. Xue, W. Wang, and B. Jha, "Persistent atmospheric and oceanic anomalies in the North Atlantic from summer 2009 to summer 2010," *Journal of Climate*, vol. 24, no. 22, pp. 5812–5830, 2011.
- [27] A. R. Lupo and P. J. Smith, "Planetary and synoptic-scale interactions during the life cycle of a mid-latitude blocking anticyclone over the North Atlantic," *Tellus A*, vol. 47, no. 5, pp. 575–596, 1995.
- [28] A. R. Lupo, "A diagnosis of two blocking events that occurred simultaneously in the midlatitude Northern Hemisphere," *Monthly Weather Review*, vol. 125, no. 8, pp. 1801–1823, 1997.
- [29] E. J. Fetzer, W. G. Read, D. Waliser et al., "Comparison of upper tropospheric water vapor observations from the Microwave Limb Sounder and Atmospheric Infrared Sounder," *Journal of Geophysical Research D*, vol. 113, no. 22, Article ID D22110, 2008.



Hindawi

Submit your manuscripts at
<http://www.hindawi.com>

